Modeling of Supercritical Extraction of Organics from Solid Matrices

Giridhar Madras, Catherine Thibaud, Can Erkey, and Aydin Akgerman
Chemical Engineering Dept., Texas A&M University, College Station, TX 77843

The desorption profiles of various organics from soil and activated carbon using dense liquid and supercritical carbon dioxide were modeled. The model accounts for effective diffusion of the organics in the solid pores, axial dispersion in the fluid phase, and external mass transfer to the fluid phase from the particle surface. This model, involving partial differential equations, is solved using the orthogonal collocation on finite elements. The model is able to predict the experimental data quite well without any adjustable parameters. The importance of each parameter depended on the system, although adsorption equilibrium and the effective pore diffusion of the organic were the most significant parameters in all the systems investigated.

Introduction

Supercritical fluids have proved to be effective solvents in regenerating solid matrices due to their unique characteristics. They have liquid-like densities, gas-like viscosities, and diffusivities at least an order of magnitude higher than that of liquids which may result in superior mass-transfer characteristics. Further, the solvent density, and hence the solvent effectiveness, can be controlled by small changes in temperature and pressure. Carbon dioxide is usually preferred as a supercritical fluid, because it is nontoxic and nonflammable, and has a low critical temperature of 304.4 K and a moderate critical pressure of 72.8 bar.

Supercritical dioxide has been used to regenerate carbon loaded with organic compounds (Modell et al., 1979; de Filippi et al., 1980; Tan and Liou, 1988, 1989a; Madras et al., 1993a) and soil loaded with heavy molecular weight organics (Dooley et al., 1987; Roop et al., 1989; Akgerman et al., 1992; Erkey et al., 1993). Other applications include purification of polymers (McHugh and Krukonis, 1986) and extraction of lignocellulosic material from wood (Li and Kiran, 1987; Goto et al., 1990).

The desorption of organics from solid matrices occurs through three consecutive mass-transport steps, which are intraparticle diffusion from the interior to the outer surface of the particle, mass transfer of the organic from the outer surface of the particle to the bulk mobile (supercritical fluid) phase and the bulk transport of the organic in the mobile phase. In addition, the thermodynamic equilibrium of the organic in the solid phase to the organic in the fluid phase plays a crucial role in the desorption process.

Many investigators (de Filippi et al., 1980; Erkey et al., 1993; Madras et al., 1993a) have employed a simple local equilibrium model, using the Freundlich isotherm and neglecting mass-transfer effects to interpret the regeneration data. This model successfully estimated the amount of carbon dioxide needed to achieve the required extraction, but could not simulate the shape of the desorption profiles accurately. Tan and Liou (1989b) investigated the desorption of ethyl acetate from carbon and proposed a single parameter model assuming linear desorption kinetics to interpret their regeneration data. Recasens et al. (1989) modeled the data of Tan and Liou (1989b) by two different parameter models: (1) an equilibrium model where the rate of desorption is controlled by external and intraparticle mass transfer; (2) a kinetic model where the external and intraparticle mass transfer and a first-order irreversible desorption step control the overall process. Later, Srinivasan et al. (1990) studied the desorption characteristics of the same system as a function of pressure, temperature, flow rate, and particle size. They modeled the system based on a well-mixed reactor and a first-order reversible desorption kinetic model. All these models, however, involve the determination of the desorption rate constant by the experimental data.

The main objective of this article is to model the desorption of heavy molecular weight organics from soil and activated carbon by supercritical carbon dioxide without the use of any adjustable parameters. Hence, we present a rigorous theoret-

---

Correspondence concerning this article should be addressed to A. Akgerman.

ical framework for the description of the regeneration of solid matrices at supercritical conditions. The other objective is to conduct a sensitivity analysis and determine the importance of each parameter in the model for the systems investigated.

Model Description

The mathematical formulation of supercritical extraction systems is similar to the formulation of adsorbers, and an extensive literature is available on adsorption processes (Yang, 1987; Ruthven, 1984). Various models have been proposed to explain the effects of operating conditions and design variables on the performance of pressure-swing adsorption (Doong and Yang, 1986; Shin and Knaebel, 1987, 1988; Matz and Knaebel, 1988).

Mathematically, the overall adsorption/desorption of the contaminant from the solid particles can be described by a set of partial differential equations (PDEs). The assumptions of the model are:

- The system is isothermal.
- The radial concentration gradients are neglected.
- The physical properties of the fluid are constant.
- The flow pattern is axially dispersed.
- There is local equilibrium in the pores.

The relevant differential fluid-phase mass balance is:

$$\frac{\partial C}{\partial \tau}-\frac{1}{Pe_b}\frac{\partial^2 C}{\partial z^2}+\frac{\partial C}{\partial z}+\frac{1-\epsilon}{\epsilon}\frac{3L}{R_p}\frac{Bi}{Pe_p}(C-c_s)=0 \tag{1}$$

The boundary conditions for this equation are given by (Smith, 1981):

$$\frac{\partial C}{\partial z}=Pe_b(C-C_o) \text{ at } z=0 \tag{1a}$$

$$\frac{\partial C}{\partial z}=0 \text{ at } z=1 \tag{1b}$$

For desorption, the initial condition is given by:

$$C=C_0 \text{ when } \tau=0 \text{ for all } z \tag{1c}$$

Assuming local equilibrium in the pores of the solid matrix, the relevant particle-phase differential mass balance is:

$$\left[\epsilon_p+(1-\epsilon_p)\frac{\partial q}{\partial c}\right]\frac{\partial c}{\partial \tau}=\frac{1}{Pe_p}\frac{L}{R_p}\frac{1}{\rho^2}\frac{\partial}{\partial \rho}\left[\rho^2\frac{\partial c}{\partial \rho}\right] \tag{2}$$

The associated boundary conditions are:

$$Bi(C-c_s)=\frac{\partial c}{\partial \rho} \text{ at } \rho=1 \tag{2a}$$

$$\frac{\partial c}{\partial \rho}=0,\ \frac{\partial q}{\partial \rho}=0 \text{ at } \rho=0 \tag{2b}$$

$$c=C_0,\ q=q_0 \text{ when } \tau=0 \text{ for all } \rho \tag{2c}$$

where q and c are related by the adsorption isotherm, $q=f(c)$. Using the Freundlich isotherm,

$$q=K\left(\frac{c}{C_{sat}}\right)^n \tag{3}$$

we have

$$\frac{dq}{dc}=\frac{Kn}{C_{sat}}\left(\frac{c}{C_{sat}}\right)^{n-1}=\frac{nq}{c} \tag{4}$$

Solution Technique

Several methods are available to solve the system of Eqs. 1-4. The most commonly used technique is the finite-difference method (Sun and Meunier, 1991), but this method requires strict conditions for stability. In the case of a linear isotherm, the system can be solved analytically by Fast Fourier Transform (Chen and Hsu, 1987), but this method cannot be applied to nonlinear isotherms. Raghavan and Ruthven (1983) used the orthogonal collocation method to solve this system of PDEs. However, as the profile along the bed gets sharper, this method fails due to numerical oscillations. A way to overcome this problem is to apply orthogonal collocation on finite elements (OCFE). OCFE technique combines the classical procedure of orthogonal collocation with the high accuracy of the finite-elements method. Since this method has been extensively described by Finlayson (1980), only an outline will be presented here.

Orthogonal collocation on finite elements

In Eqs. 1 and 2, the variables z and ρ take values in the interval [0, 1]. In the z direction, the interval is divided into N_{el} equally-spaced finite elements by fixing $(N_{el}-1)$ internal node points, Z_k for $k=1, \ldots N_{el}-1$, and we will denote $Z_0=0$ and $Z_{Nel}=1$. The length of each finite element is:

$$L_{el}=\frac{1}{N_{el}} \tag{5}$$

Orthogonal collocation is applied inside each finite element which requires the normalization of the variable in each element. The normalized variable in each element is given by:

$$s_k=\frac{z-Z_{k-1}}{L_{el}} \tag{6}$$

Only one element is considered in the radial direction for each particle, since a relatively simple profile is expected in the particle. In each element, orthogonal collocation points are calculated as roots of given polynomials and at each collocation point, the first derivative and the Laplacian of the unknown function (organic concentration) are discretized using discretization matrices A and B which can be calculated from the collocation points (Finlayson, 1980). In the axial direction, NP interior collocation points are considered and Legendre polynomials are used. In the radial direction (inside the soil particles), NR interior collocation points are considered and Jacobi polynomials in ρ^2 are used to take advantage of the problem symmetry (Finlayson, 1980). This ensures that the condition at the center of the particle is automatically satisfied.

The orthogonal collocation on finite-elements method transforms the system of PDEs (Eqs. 1-2) into a system of algebraic differential equations (ADEs) where the unknowns are the concentrations at each node point. The concentration at each grid point is denoted as shown in Figure 1. The bulk-phase concentration corresponding to the ith point in the kth finite element is denoted by C_i^k, and the pore phase concentration corresponding to the jth point is denoted by $c_j^{i,k}$, where i and k have the same meaning as before.

At each interior collocation point (z or ρ direction), the corresponding differential equation (Eq. 1 or 2) is supposed to be satisfied:

At each z-direction interior collocation point:

$$\frac{dC_i^k}{d\tau}-\frac{1}{Pe_b}\frac{1}{L_{el}^2}\left[\sum_{l=1}^{l=NP+2} BZ_{i,l}C_l^k\right]+\frac{1}{L_{el}}\left[\sum_{l=1}^{l=NP+2} AZ_{i,l}C_l^k\right]+\frac{1-\epsilon}{\epsilon}\frac{3L}{R_p}\frac{Bi}{Pe_p}\left(C_i^k-c_{NR+1}^{i,k}\right)=0 \qquad (7)$$

for all $i=2, 3, \ldots, NP+1$ and for all $k=1, 2, \ldots N_{el}$

At each ρ-direction interior collocation point:

$$\left[\epsilon_p+(1-\epsilon_p)f'\left(c_j^{i,k}\right)\right]\frac{dc_j^{i,k}}{d\tau}-\frac{1}{Pe_p}\frac{L}{R_p}\left[\sum_{l=1}^{l=NR+1} BR_{j,l}c_l^{i,k}\right]=0 \qquad (8)$$

for all $i=1, 2, \ldots NP+2$, for all $k=1, 2, \ldots N_{el}$, and for all $j=1, 2, \ldots NR$, where $f'(c)$ is defined by Eq. 4.

The associated boundary conditions are:

Bed inlet: $z=Z_0=0$

$$\frac{1}{L_{el}^2}\left[\sum_{l=1}^{l=NP+2} AZ_{1,l}C_l^1\right]-Pe_b\left(C_1^1-C_o\right)=0 \qquad (8a)$$

Bed exit: $z=Z_{N_{el}}=1$

$$\frac{1}{L_{el}}\left[\sum_{l=1}^{l=NP+2} AZ_{NP+2,l}C_l^{N_{el}}\right]=0 \qquad (8b)$$

An additional boundary condition at the surface of the particle ($\rho=1$) is given by:

$$\left[\sum_{l=1}^{l=NR+1} AR_{NR+1,l}c_l^{i,k}\right]-Bi\left(C_i^k-c_{NR+1}^{i,k}\right)=0 \qquad (8c)$$

for all $i=1, 2, \ldots NP+2$ and for all $k=1, 2, \ldots N_{el}$.

Between each finite element ($z=Z_k$, $k=1, 2, \ldots N_{el}-1$), continuity of the flux is imposed:

$$\left[\sum_{l=1}^{l=NP+2} AZ_{NP+2,l}C_l^k\right]-\left[\sum_{l=1}^{l=NP+2} AZ_{1,l}C_l^{k+1}\right]=0 \qquad (9)$$

It has to be noted that:

$$C_{NP+2}^k=C_1^{k+1} \text{ for all } k=1, 2, \ldots, N_{el} \qquad (9a)$$

The initial condition is:

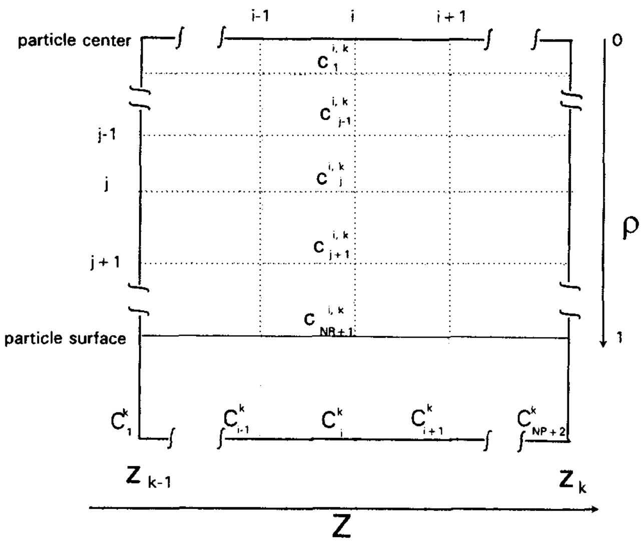

Figure 1. Location of collocation points and nomenclature for grid points in kth finite element.

$$\text{at } \tau=0,\ C_i^k=c_j^{i,k}=C_0 \text{ for all } i, j, k \qquad (9b)$$

Equations 8-10 form a system of $[N_{el}(NP+1)+1](NR+2)$ ADEs with $[N_{el}(NP+1)+1](NR+2)$ unknowns which can be written under the form:

$$\alpha\frac{du}{d\tau}+\beta u=0 \qquad (10)$$

with initial condition:

$$\text{at } \tau=0,\ u=u_0 \qquad (10a)$$

where u is the vector containing the values of the contaminant concentration at each grid point. Following Yu and Wang (1985), the grid points were numbered in a particular way to reduce the bandwidth of the matrix β and decrease the computational time. This system was solved by the code DASSL (Petzold, 1982) on the DEC-VAX 9000 computer and the Cray-YMP supercomputer. This code uses backward differentiation formulas to advance the solution from one time step to the next.

DASSL requires a consistent set of initial values $\{u\}$ and $\{du/d\tau\}$. It is then necessary to modify the initial condition to have a continuous change in the inlet concentration. Following Lu et al. (1992), the initial negative step change was approximated by the function:

$$C_o=C_0\exp(-s\tau) \qquad (11)$$

with $s=10^{10}$.

Parameter Identification and Correlations

The parameters involved in the model are the mass-transfer coefficient to the bulk phase, axial dispersion coefficient in the fluid phase, and effective pore diffusivity in the particle and the adsorption equilibrium parameters, K and n. These parameters were evaluated using existing correlations and available data.

The mass-transfer coefficient was estimated using the empirical correlation reported by numerous workers (Wakao, 1982):

$$Sh = 2 + 1.1Sc^{\frac{1}{3}}Re^{0.6} \tag{12}$$

This correlation was developed for conventional processes, but it has been successfully used for supercritical extraction (Brunner, 1985).

The axial dispersion coefficients in supercritical carbon dioxide in packed beds were measured by Tan and Liou (1989c). They proposed an empirical correlation involving nondimensionless groups, which generated their data with an average deviation of 8.5%. Correlations based on dimensionless groups such as

$$Pe_{pd} = 0.817Re^{0.265}Sc^{-0.919} \tag{13}$$

showed an average deviation of 21% from the data of Tan and Liou (1989c). However, since correlations based on dimensionless groups are useful for scaleup of processes, we used the above correlation (Eq. 13) to evaluate the axial dispersion in supercritical carbon dioxide.

The effective pore diffusivity in the particle is given by:

$$D_p = \frac{\epsilon_p}{\tau_p} D_m \tag{14}$$

where D_m is the diffusion coefficient of the organic in the supercritical fluid, and τ_p is the tortuosity factor (Smith, 1981). The tortuosity factor of solids is usually in the range of 2–8 and was held constant at a value of 3 for all the cases investigated in this study. Orejuela (1994) has used the Taylor dispersion technique to determine the diffusion coefficients of heavy molecular weight organics in supercritical carbon dioxide. The particle porosities of soil and carbon, evaluated using the nitrogen desorption technique, were 0.12 and 0.39, respectively. Effective pore diffusivities were evaluated using the values of molecular diffusivities, particle porosities, and tortuosity.

Adsorption equilibrium

At equilibrium, the distribution of the organic between the solid phase and the supercritical phase is determined by the adsorption isotherm. We have determined the adsorption isotherms of heavy molecular organics both on soil and on activated carbon using a technique based on frontal analysis chromatography. In this technique, a positive step change in the concentration of the solute is imposed at the inlet of the bed and the effluent concentration is monitored to obtain a breakthrough curve. Analysis of the breakthrough curves obtained at various inlet concentrations yields the adsorption isotherm. The experimental apparatus, procedure, operating conditions used for the adsorption and desorption experiments have been detailed by Erkey et al. (1993) and Madras et al. (1993a). The adsorbates employed were naphthalene, phenanthrene, hexachlorobenzene, and pentachlorophenol; the adsorbents were soil and activated carbon; and the solvent used for regeneration was supercritical carbon dioxide. The adsorption isotherms of these organics on soil and carbon in dense liquid and supercritical carbon dioxide were modeled by the Freundlich isotherm, given by Eq. 3. The Freundlich constants, K and n, are summarized in Table 1. The saturation concentrations (solubilities) of the organics in supercritical carbon dioxide, C_{sat}, are given in Table 2. These solubilities were measured by a new technique developed by Madras et al. (1993b).

The densities of supercritical carbon dioxide were evaluated from IUPAC (1976), and the viscosities were interpolated from the data of Tan and Liou (1989c). The bed porosity, evaluated by injecting an inert tracer through the packed bed, was 0.5. The parameters, k_f, D_L, and D_p, evaluated from the above correlations, as well as data on D_m from Orejuela (1994), are tabulated in Table 3.

Desorption Experiments

Prior to desorption, the organic was at equilibrium between

Table 1. Freundlich Constants for the Organics

Solute	Solid	Freundlich Constants	298 K	308 K	318 K	328 K
Naphthalene	Soil	K, mg/g		3.78	5.06	6.23
		n		1	1	1
	Carbon	K, mg/g		245.5	257.04	
		n		0.2	0.2	
Phenanthrene	Soil	K, mg/g		2.14	2.75	3.84
		n		1	1	1
	Carbon	K, mg/g		158.48	288.40	
		n		0.14	0.22	
Hexachlorobenzene	Soil	K, mg/g	0.17	0.20	0.42	
		n	1	1	1	
	Carbon	K, mg/g		169.82	223.87	
		n		0.23	0.19	
Pentachlorophenol	Soil	K, mg/g	11.58	13.57	20.69	
		n	0.91	0.75	0.56	
	Carbon	K, mg/g		288.4	338.8	
		n		0.24	0.22	

Table 2. Saturation Concentration, C_{sat}, of the Organics in Carbon Dioxide

Solute	Temp. K	Pres. atm	C_{sat} mmol/L
Naphthalene	308	100	171.8
	318	100	86.3
	328	100	22.2
Phenanthrene	308	100	9.67
	318	100	5.04
	328	100	1.31
Hexachlorobenzene	298	113	0.695
	308	113	0.576
	318	113	0.509
Pentachlorophenol	298	113	2.95
	308	113	2.71
	318	113	2.24

the adsorbent and the supercritical phase. The concentration of the organic in the fluid phase in the packed bed corresponds approximately to 95% of the solubility of the organic in the fluid phase at the experimental conditions. The desorption profiles were obtained by passing pure carbon dioxide through this packed bed of soil or carbon. In all the cases, the flow rate was maintained at 200 mL/h at the pump conditions. This was converted to the interstitial velocities at the column conditions by using the appropriate densities and the bed dimensions in Table 4. These experiments are described extensively by Erkey et al. (1993) and Madras et al. (1993a).

Table 4. Dimensions of the Packed Bed

Solute	Solid	Bed Dia., m	Bed Length, m
Naphthalene	Soil	0.0046	0.25
	Carbon	0.0046	0.25
Phenanthrene	Soil	0.0046	0.25
	Carbon	0.0021	0.05
Hexachlorobenzene	Soil	0.01	0.25
	Carbon	0.0021	0.05
Pentachlorophenol	Soil	0.0021	0.20
	Carbon	0.0021	0.05

Results and Discussion

The experimental desorption profiles were compared with the desorption profiles predicted by the above model (Eqs. 1-2), using the parameters in Tables 1-4 (Figures 2-9). For clarity, some of the desorption profiles have been plotted as relative fluid-phase concentration, C/C_{sat} vs. time, while others represent the variation of the fluid-phase concentration, C, vs. time. The agreement between the model predictions and the experimental data is acceptable considering that the model involves no adjustable parameters. For some systems, however, the tail of the desorption profile could not be accurately modeled (Figures 3-5, 8, and 9).

Theoretically, the long tail observed in the desorption profiles can be attributed to axial dispersion, mass-transfer resistance, and/or to nonlinearity of the adsorption isotherm. To determine which one of these parameters actually controls

Table 3. Parameters Evaluated from Correlations and Data

Solute	Solid	Parameters	298 K	308 K	318 K	328 K
Naphthalene	Soil	$D_p \times 10^{10}$, m^2/s		5.88	6.8	8.4
		$D_m \times 10^{8}$, m^2/s		1.47	1.75	2.1
		$D_L \times 10^{6}$, m^2/s		3.54	3.6	4.6
		$k_f \times 10^{3}$, m/s		1.31	1.71	2.4
	Carbon	$D_p \times 10^{10}$, m^2/s		20.5	23.7	
		$D_m \times 10^{8}$, m^2/s		1.47	1.75	
		$D_L \times 10^{6}$, m^2/s		2.12	2.16	
		$k_f \times 10^{3}$, m/s		0.91	1.18	
Phenanthrene	Soil	$D_p \times 10^{10}$, m^2/s			6.4	9.2
		$D_m \times 10^{8}$, m^2/s			1.6	2.3
		$D_L \times 10^{6}$, m^2/s			3.81	4.23
		$k_f \times 10^{3}$, m/s			1.64	2.58
	Carbon	$D_p \times 10^{10}$, m^2/s		14.3	20.8	
		$D_m \times 10^{8}$, m^2/s		1.13	1.6	
		$D_L \times 10^{6}$, m^2/s		8.78	7.25	
		$k_f \times 10^{3}$, m/s		1.74	2.68	
Hexachlorobenzene	Soil	$D_p \times 10^{10}$, m^2/s	4		6	
		$D_m \times 10^{8}$, m^2/s	1		1.25	
		$D_L \times 10^{6}$, m^2/s	1.15		1.37	
		$k_f \times 10^{3}$, m/s	0.34		0.59	
	Carbon	$D_p \times 10^{10}$, m^2/s		14.3	16.2	
		$D_m \times 10^{8}$, m^2/s		1.1	1.25	
		$D_L \times 10^{6}$, m^2/s		9.07	8.15	
		$k_f \times 10^{3}$, m/s		1.73	2.15	
Pentachlorophenol	Soil	$D_p \times 10^{10}$, m^2/s	3.2		4.4	
		$D_m \times 10^{8}$, m^2/s	0.8		1.1	
		$D_L \times 10^{6}$, m^2/s	11.9		9.17	
		$k_f \times 10^{3}$, m/s	1.29		1.97	
	Carbon	$D_p \times 10^{10}$, m^2/s		12.9	14.3	
		$D_m \times 10^{8}$, m^2/s		0.99	1.1	
		$D_L \times 10^{6}$, m^2/s		9.9	9.17	
		$k_f \times 10^{3}$, m/s		1.62	1.97	

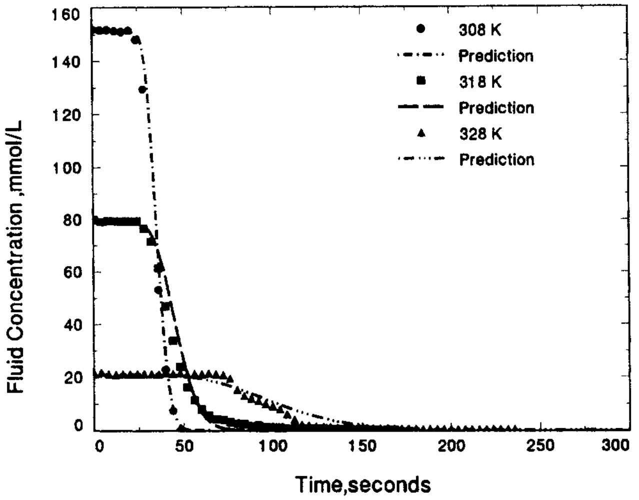

Figure 2. Desorption profile of naphthalene from soil at 100 atm.

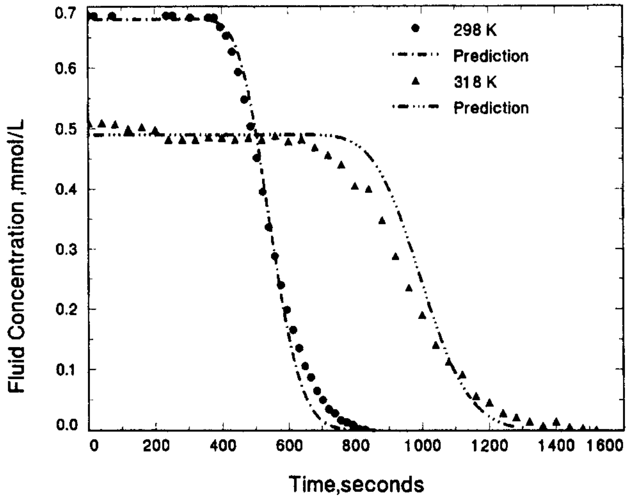

Figure 4. Desorption profile of hexachlorobenzene from soil at 113 atm.

the shape of the desorption profile, a sensitivity analysis was performed on the adsorption equilibrium parameters and the rate parameters.

The adsorption isotherms of organics on activated carbon were modeled by a Freundlich isotherm (Eq. 3). The sensitivity analysis on the adsorption equilibrium parameters, *n* and *K*, was performed by changing by a factor of two the value of the exponent, *n*, obtained by fitting the experimental data. The value of the parameter *K* was changed accordingly, so that the initial contamination level remained constant. The adsorption isotherms of hexachlorobenzene on carbon at 308 K obtained with the modified values of *n* and *K* are shown in Figure 10 together with the experimental isotherm. It has to be noted that the initial slopes are very much affected by a change in the value of the isotherm's parameter *n*. The desorption profile was evaluated using each isotherm. As shown in Figure 11, the change in the value of *n* produced a significant change in the desorption profile.

To determine the importance of the rate parameters, the

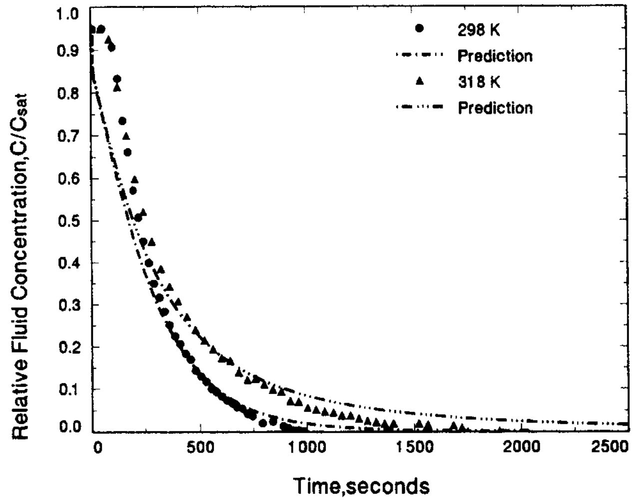

Figure 5. Desorption profile of pentachlorophenol from soil at 113 atm.

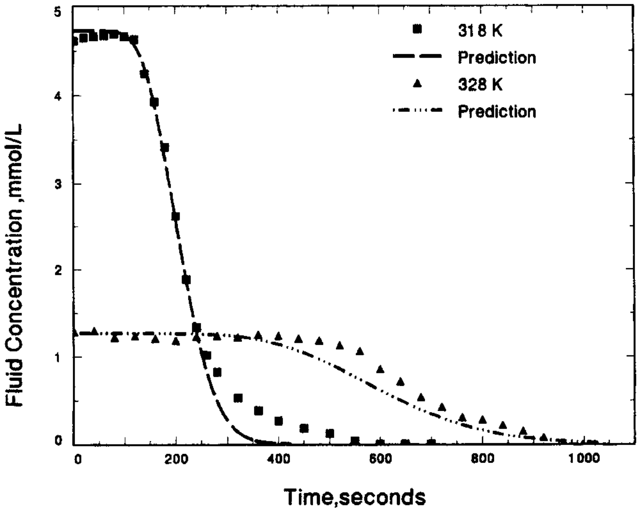

Figure 3. Desorption profile of phenanthrene from soil at 100 atm.

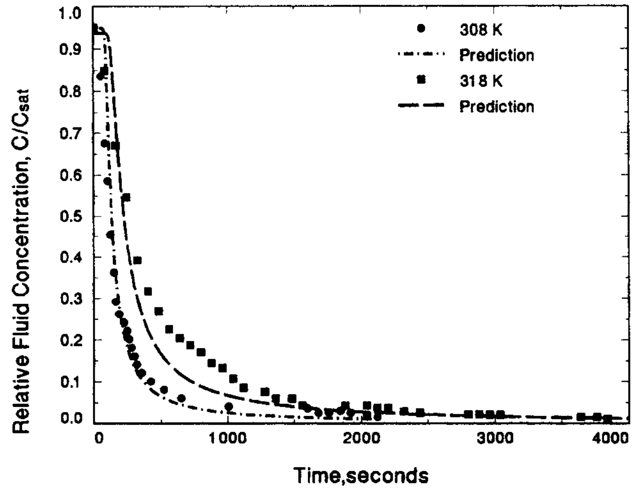

Figure 6. Desorption profile of naphthalene from carbon at 100 atm.

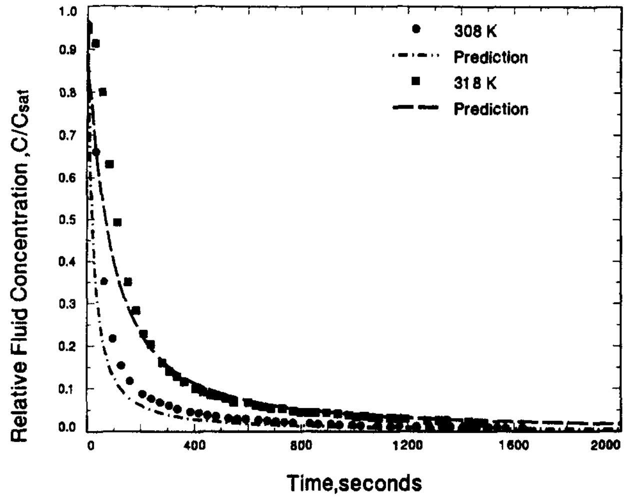

Figure 7. Desorption profile of phenanthrene from carbon at 113 atm.

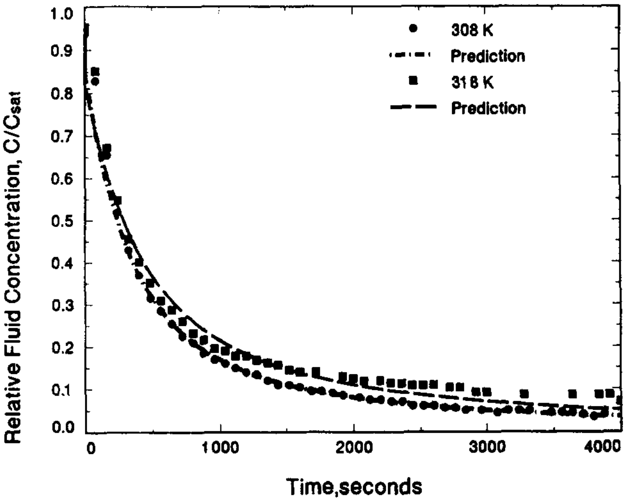

Figure 8. Desorption profile of hexachlorobenzene from carbon at 113 atm.

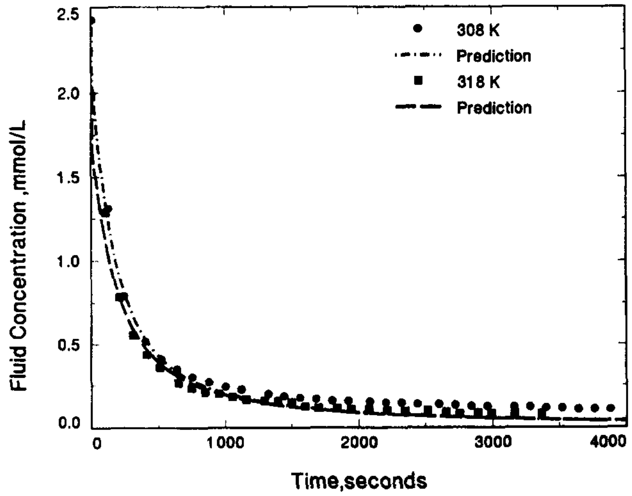

Figure 9. Desorption profile of pentachlorophenol from carbon at 113 atm.

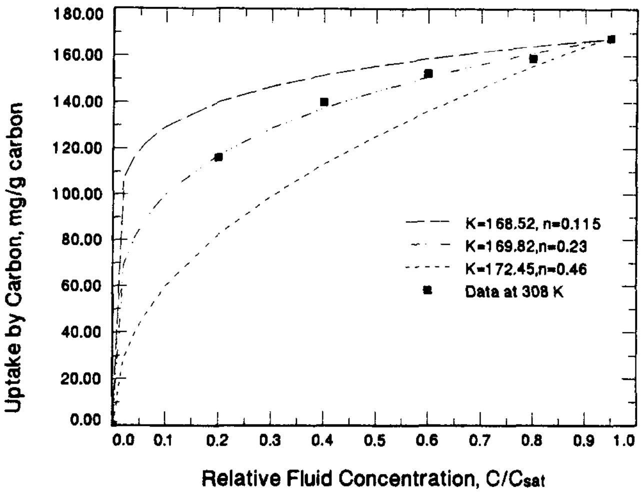

Figure 10. Adsorption isotherm of hexachlorobenzene on carbon at 308 K and 113 atm with various values of *K* and *n*.

sensitivity of the model to each rate parameter (k_f, D_L, and D_p) was assessed by reevaluating the desorption profile after changing the parameter's value by an order of magnitude around the value obtained by correlations (Eqs. 12–14). The results obtained for desorption of hexachlorobenzene from carbon at 308 K are shown in Figure 12. A change in the effective diffusivity's value produced an appreciable change in the initial portion and a small change in the tail of the desorption profile (Figure 12), but an order of magnitude change on the values of other parameters, k_f and D_L, produced no appreciable change in the desorption profile. This indicates that, for this system, the effect of the mass transfer of the organic from the particle to the bulk phase (parameter k_f) and axial dispersion of the organic in the fluid phase (parameter D_L) are negligible compared to the effect of the organic's diffusion in the pores (parameter D_p) and adsorption equilibrium. However, as the change in the desorption profiles produced by the perturbation on the adsorption equilibrium

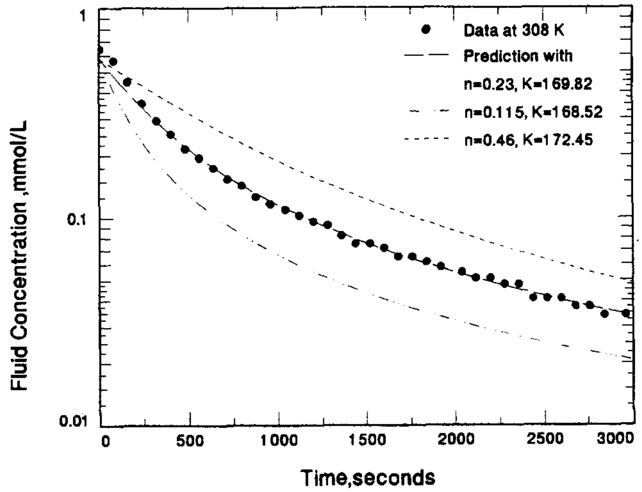

Figure 11. Sensitivity analysis of adsorption parameters on the desorption profile of hexachlorobenzene from carbon at 308 K and 113 atm.

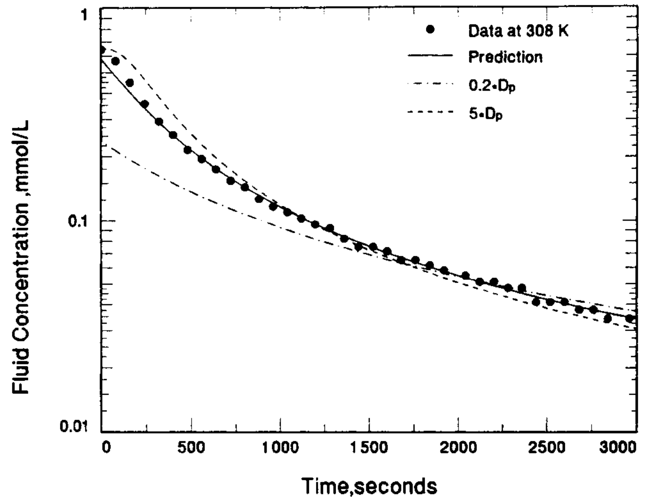

Figure 12. Sensitivity analysis of rate parameters on the desorption profile of hexachlorobenzene from carbon at 308 K and 113 atm.

parameters is more significant than the change due to a perturbation on the effective diffusivity, we can conclude that the long tails observed in the desorption profiles of organics from carbon can be attributed to the shape of the adsorption isotherm and especially to the steepness of the slopes in the initial portion of the adsorption isotherm. In the cases investigated, only few experimental points were available in the initial portion of the adsorption isotherm, and the values of n and K could not be precisely estimated which explains the lack of accuracy in the prediction of the tail of the desorption profiles (Figures 8 and 9). Emergence of the adsorption isotherm's parameters as the crucial parameters for the accurate prediction of the desorption profiles of organics from activated carbon is consistent with the successful implementations of the local equilibrium theory (which assumes plug flow and negligible mass-transfer resistances) for the desorption of organics from carbon, as reported by Modell (1979) and Madras (1993a).

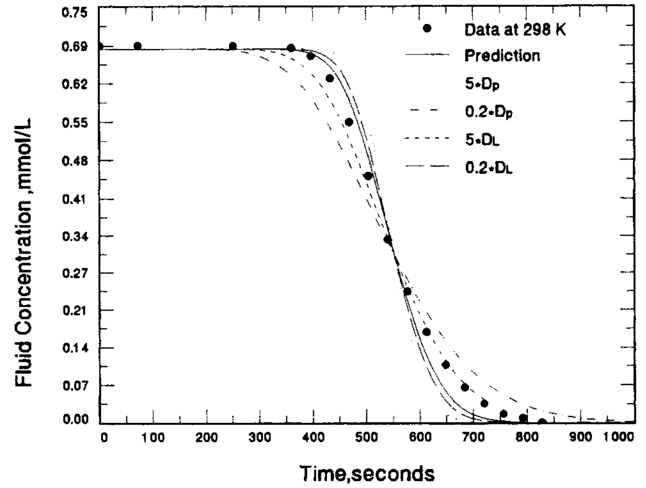

Figure 13. Sensitivity analysis of rate parameters on the desorption profile of hexachlorobenzene from soil at 308 K and 113 atm.

The tailing of the desorption profiles of organics from soil (Figures 2–5) cannot be attributed to the adsorption isotherm, since the adsorption isotherm is linear in most of the investigated cases (Erkey et al., 1993). The local equilibrium theory has proved unsuccessful in determining the shape of the desorption profile of organics from soil, since it predicts a perfect step in the desorption profile (Erkey et al., 1993). That is why the tailing of the desorption profiles has to be attributed to the rate parameters. To investigate the effect of the rate parameters on the desorption of organics from soil, a perturbation analysis was conducted on the hexachlorobenzene–soil system at 298 K. While a perturbation of the parameters, D_L and D_p, had a significant effect on the desorption profile as shown in Figure 13, an order of magnitude change on the mass-transfer coefficient, k_f, did not produce any change in the shape of the desorption profile. However, caution has to be exercised when generalizing this result to other systems and particle Reynolds numbers have to be compared. As reported by Srinivasan et al. (1990) and Recasens et al. (1989), if the flow rate of supercritical carbon dioxide is very low (low particle Reynolds number), mass transfer may play an important role in the desorption process. The particle Reynolds numbers used in our experiments were at least an order of magnitude greater than those used in the experiments of Srinivasan et al. (1990), and the external mass-transfer coefficients evaluated from Eq. 12 for our experiments were at least an order of magnitude larger than the value of k_f obtained by Srinivasan et al. (1990) with the same correlation.

Thus, the importance of each parameter depends on the system being investigated, and care must be taken in postulating the simplifying assumptions regarding the importance of each parameter on a case-by-case basis. However, provided the adsorption isotherm and the molecular diffusivity data are available, the desorption profiles of the organics from solid matrices in presence of supercritical fluids can be predicted fairly well with no adjustable parameters, using the correlations given by Eqs. 12–14.

Acknowledgment

This project was funded through grants CTS-902206 from the National Science Foundation and 100TAM0087 and 111TAM2087 from the Gulf Coast Hazardous Substance Research Center. Their contributions are greatly appreciated.

Notation

AR = collocation matrix for gradient with Jacobi polynomials
AZ = collocation matrix for gradient with Legendre polynomials
BR = collocation matrix for Laplacian with Jacobi polynomials
BZ = collocation matrix for Laplacian with Legendre polynomials
c = sorbate concentration in the particle pore
c_s = sorbate concentration at the surface of the particle
C = sorbate concentration in the bulk phase
C_{sat} = saturation concentration in the bulk phase
D_L = axial dispersion coefficient
D_m = molecular diffusion coefficient
D_p = effective diffusivity in the particle pore
f = isotherm functionality, $q=f(c)$
f' = first derivative of the isotherm
K = Freundlich constant
k_f = mass-transfer coefficient
L = length of the bed
n = exponent in the Freundlich isotherm
NR = number of interior collocation points in the ρ direction
NP = number of node interior collocation points in the z direction

q = sorbate concentration in the particle solid phase
r = axial coordinate in the particle
R_p = particle radius
t = time
u = vector of concentration at node point
v = interstitial fluid velocity
x = distance measured from bed inlet
Z = finite element's frontier point

Dimensionless variables and parameters

s = dimensionless axial coordinate in each finite element
z = dimensionless axial coordinate along the bed, x/L
ρ = dimensionless radial coordinate in the particle, r/R_p
τ = dimensionless time, $(tv)/L$
Bi = Biot number, $(k_f R_p)/D_p$
Pe_b = Peclet number for the bed, $(Lv)/D_L$
Pe_p = Peclet number for the particle, $(R_p v)/D_p$
Pe_{pd} = Peclet number for the particle, $(R_p v)/D_L$
Sc = Schmidt number, $\mu_f/(\rho_f D_m)$
Re = Reynolds number, $(2\ R_p v \rho_f)/\mu_f$
Sh = Sherwood number, $(2\ R_p k_f)/D_p$

Greek letters

ϵ = void fraction of bed
ϵ_p = void fraction of particle
τ_p = tortuosity
μ_f = fluid viscosity
ρ_f = fluid density
α, β = ADE system matrices

Subscripts

0 = time $t=0$
el = element
o = bed inlet
s = surface of the particle

Literature Cited

Akgerman, A. C., C. Erkey, and S. M. Ghoreishi, "Supercritical Extraction of Hexachlorobenzene from Soil," *Ind. Eng. Chem. Res.*, **31**, 333 (1992).

Brunner, G., "Mass Transfer in Gas Extraction," *Supercritical Fluid Technology*, p. 245, J. M. L. Penniger, M. Radosz, M. A. McHugh, V. J. Krukonis, eds., Elsevier, Amsterdam (1985).

Chen, T. L., and J. T. Hsu, "Prediction of Breakthrough Curves by the Application of Fast Fourier Transform," *AIChE J.*, **33**, 1387 (1987).

de Filippi, R. P., V. J. Krukonis, R. J. Robey, and M. Modell, "Supercritical Fluid Regeneration of Activated Carbon for Adsorption of Pesticides," EPA Report, Washington, DC (1980).

Dooley, B. O., C. Kao, R. P. Gambrell, and F. C. Knopf, "The Use of Entrainers in the Supercritical Extraction of Soils Contaminated With Hazardous Organics," *Ind. Eng. Chem. Res.*, **26**, 2058 (1987).

Doong, S. J., and R. T. Yang, "Bulk Separation of Multicomponent Gas Mixtures by Pressure Swing Adsorption: Pore/Surface Diffusion and Equilibrium Models," *AIChE J.*, **32**, 397 (1986).

Erkey, C., G. Madras, M. Orejuela, and A. Akgerman, "Supercritical Carbon Dioxide Regeneration of Organics From Soil," *Environ. Sci. Technol.*, **27**, 1225 (1993).

Finlayson, B. A., *Nonlinear Analysis in Chemical Engineering*, McGraw Hill, New York (1980).

Goto, M., J. M. Smith, and B. J. McCoy, "Kinetics and Mass Transfer for Supercritical Fluid Extraction," *Ind. Eng. Chem. Res.*, **29**, 282 (1990).

IUPAC, "International Thermodynamic Tables of the Fluid State Carbon Dioxide," S. Angus, B. Armstrong, and K. M. de Reuck, eds., Pergamon Press, New York (1976).

Li, L., and E. Kiran, "A Kinetic Model for Supercritical Delignification of Wood," AIChE Meeting, Washington, DC (1988).

Lu, Z., J. M. Loureiro, M. D. LeVan, and A. E. Rodriques, "Effect of Intraparticle Forced Convection on Gas Desorption from Fixed Beds Containing 'Large-Pore' Adsorbents," *Ind. Eng. Chem. Res.*, **31**, 1530 (1992).

Madras, G., C. Erkey, and A. Akgerman, "Supercritical Fluid Regeneration of Carbon Loaded with Heavy Molecular Weight Organics," *Ind. Eng. Chem. Res.*, **32**, 1163 (1993a).

Madras, G., C. Erkey, and A. Akgerman, "A New Technique for Measuring Solubilities of Organics in Supercritical Fluids," *J. Chem. Eng. Data*, **38**, 422 (1993b).

Matz, M. J., and K. S. Knaebel, "Pressure Swing Adsorption: Effects of Incomplete Purge," *AIChE J.*, **34**, 1486 (1988).

McHugh, M. A., and V. J. Krukonis, *Supercritical Fluid Extraction: Principles and Practice*, Butterworths, Stoneham, MA (1986).

Modell, M., R. J. Robey, V. J. Krukonis, R. D. de Fillipi, and D. Oestereich, "Supercritical Fluid Regeneration of Activated Carbon," AIChE Meeting, Boston (1979).

Orejuela, M., "Limiting Diffusion Coefficients of Heavy Molecular Weight Organics in Supercritical Carbon Dioxide," MS Thesis, Texas A&M Univ. (1994).

Petzold, L. R., "A Description of DASSL: a Differential/Algebraic Equation System Solver," STR, SAND82-8637, Livermore (1982).

Raghavan, N. S., and D. M. Ruthven, "Numerical Simulation of a Fixed Bed Adsorption Column by the Method of Orthogonal Collocation," *AIChE J.*, **29**, 922 (1983).

Recasens, F., J. M. Smith, and B. J. McCoy, "Desorption Processes: Supercritical Fluid Regeneration of Activated Carbon," *AIChE J.*, **35**, 951 (1989).

Roop, R. K., R. K. Hess, and A. Akgerman, "Supercritical Extraction of Priority Pollutants From Water and Soil," *Supercritical Fluid Science and Technology*, K. P. Johnston and J. M. L. Penniger, eds., Amer. Chem. Soc., Washington, DC (1989).

Ruthven, D. M., *Principles of Adsorption and Adsorption Processes*, Wiley, New York (1984).

Shin, H. S., and K. S. Knaebel, "Pressure Swing Adsorption: A Theoretical Study of Diffusion Induced Separation," *AIChE J.*, **33**, 654 (1987).

Shin, H. S., and K. S. Knaebel, "Pressure Swing Adsorption: An Experimental Study of Diffusion Induced Separation," *AIChE J.*, **34**, 1409 (1988).

Smith, J. M., *Chemical Engineering Kinetics*, McGraw-Hill, New York (1981).

Srinivasan, M. P., J. M. Smith, and B. J. McCoy, "Supercritical Fluid Desorption from Activated Carbon," *Chem. Eng. Sci.*, **45**, 1885 (1990).

Sun, L. M., and F. Meunier, "An Improved Finite Difference Method for Fixed-bed Multicomponent Adsorption," *AIChE J.*, **37**, 244 (1991).

Tan, C. S., and D. C. Liou, "Desorption of Ethyl Acetate from Activated Carbon by Supercritical Carbon Dioxide," *Ind. Eng. Chem. Res.*, **27**, 988 (1988).

Tan, C. S., and D. C. Liou, "Supercritical Regeneration of Activated Carbon Loaded with Benzene and Toluene," *Ind. Eng. Chem. Res.*, **28**, 1222 (1989a).

Tan, C. S., and D. C. Liou, "Modeling of Desorption at Supercritical Conditions," *AIChE J.*, **35**, 1029 (1989b).

Tan, C. S., and D. C. Liou, "Axial Dispersion of Supercritical Carbon Dioxide in Packed Beds," *Ind. Eng. Chem. Res.*, **28**, 1246 (1989c).

Wakao, N., and S. Kaguei, *Heat and Mass Transfer in Packed Beds*, Gordon and Breach, New York (1982).

Yang, R. T., *Gas Separation by Adsorption Processes*, Butterworths, Boston (1987).

Yu, Q., and N. H. L. Wang, "Computer Simulations of the Dynamics of Multicomponent Ion Exchange and Adsorption in Fixed Beds—Gradient-Directed Moving Finite Element Method," *Comp. Chem. Eng.*, **13**(8), 915 (1989).

Manuscript received May 11, 1993, and revision received Aug. 2, 1993.